



## OpenAIR@RGU

### The Open Access Institutional Repository at Robert Gordon University

<http://openair.rgu.ac.uk>

This is an author produced version of a paper published in

Energy (ISSN 0360-5442)

This version may not include final proof corrections and does not include published layout or pagination.

#### Citation Details

##### Citation for the version of the work held in 'OpenAIR@RGU':

**ABU-BAKAR, S. H., MUHAMMAD-SUKKI, F., FREIER, D., RAMIREZ-INIGUEZ, R., MALLICK, T. K., MUNIR, A. B., YASIN, S. H. M., MAS'UD, A. A. and BANI, N. A., 2016. Performance analysis of a solar window incorporating a novel rotationally asymmetrical concentrator. Available from *OpenAIR@RGU*. [online]. Available from: <http://openair.rgu.ac.uk>**

##### Citation for the publisher's version:

**ABU-BAKAR, S. H., MUHAMMAD-SUKKI, F., FREIER, D., RAMIREZ-INIGUEZ, R., MALLICK, T. K., MUNIR, A. B., YASIN, S. H. M., MAS'UD, A. A. and BANI, N. A., 2016. Performance analysis of a solar window incorporating a novel rotationally asymmetrical concentrator. *Energy*, Vol. 99, pp. 181-192.**



**This work is licensed under a Creative Commons Attribution - Non-Commercial - No-Derivatives 4.0 International Licence**

#### Copyright

Items in 'OpenAIR@RGU', Robert Gordon University Open Access Institutional Repository, are protected by copyright and intellectual property law. If you believe that any material held in 'OpenAIR@RGU' infringes copyright, please contact [openair-help@rgu.ac.uk](mailto:openair-help@rgu.ac.uk) with details. The item will be removed from the repository while the claim is investigated.

© 2016. This manuscript version is made available under the CC-BY-NC-ND 4.0 license <http://creativecommons.org/licenses/by-nc-nd/4.0/>

<http://dx.doi.org/10.1016/j.energy.2016.01.006>

# Performance analysis of a solar window incorporating a novel rotationally asymmetrical concentrator

Siti Hawa Abu-Bakar<sup>a,b,\*</sup>, Firdaus Muhammad-Sukki<sup>c,d</sup>, Daria Freier<sup>a</sup>, Roberto Ramirez-Iniguez<sup>a</sup>, Tapas Kumar Mallick<sup>e</sup>, Abu Bakar Munir<sup>f,g</sup>, Siti Hajar Mohd Yasin<sup>h</sup>, Abdullahi Abubakar Mas'ud<sup>i</sup>, Nurul Aini Bani<sup>j</sup>

<sup>a</sup> School of Engineering & Built Environment, Glasgow Caledonian University, 70 Cowcaddens Road, Glasgow, G4 0BA Scotland, United Kingdom

<sup>b</sup> Universiti Kuala Lumpur British Malaysian Institute, Batu 8, Jalan Sungai Pusu, 53100 Gombak, Selangor, Malaysia

<sup>c</sup> School of Engineering, Faculty of Design and Technology, Robert Gordon University, Garthdee House, Garthdee Road, Aberdeen, AB10 7QB, Scotland, United Kingdom

<sup>d</sup> Faculty of Engineering, Multimedia University, Persiaran Multimedia, 63100 Cyberjaya, Selangor, Malaysia

<sup>e</sup> Environment and Sustainability Institute, University of Exeter, Penryn, Cornwall, TR10 9EZ, United Kingdom

<sup>f</sup> Faculty of Law, University of Malaya, 50603 Kuala Lumpur, Malaysia

<sup>g</sup> University of Malaya Malaysian Centre of Regulatory Studies (UMCoRS), University of Malaya, 59990 Jalan Pantai Baru, Kuala Lumpur, Malaysia

<sup>h</sup> Faculty of Law, Universiti Teknologi MARA, 40450 Shah Alam, Malaysia

<sup>i</sup> Department of Electrical and Electronic Engineering Technology, Jubail Industrial College, P O Box 10099, Saudi Arabia

<sup>j</sup> UTM Razak School of Engineering and Advanced Technology, Universiti Teknologi Malaysia, 54100 Kuala Lumpur, Malaysia

\* Phone/Fax number: +44(0)141 273 1482/+44(0)141 331 3690, e-mail: [sitihawa.abubakar@gcu.ac.uk](mailto:sitihawa.abubakar@gcu.ac.uk)/[hawa012@gmail.com](mailto:hawa012@gmail.com)

**Abstract:** The race towards achieving a sustainable zero carbon building has spurred the introduction of many new technologies, including the building integrated photovoltaic (BIPV) system. To tackle the high capital cost of BIPV systems, low-concentration photovoltaic (LCPV) technology was developed. Besides the reduction of cost, the LCPV technology also produces clean energy for the building and promotes innovative architectural design. This paper presents a novel type of concentrator for BIPV systems. This concentrator, known as the *rotationally asymmetrical dielectric totally internally reflecting concentrator* (RADTIRC), was incorporated in a small double glazing window. The RADTIRC has a geometrical concentration ratio of 4.9069x. A series of experiments were carried out to evaluate the performance of the solar PV window both indoors and outdoors. It was found that the RADTIRC-PV window increases the short circuit current by 4.13x when compared with a non-concentrating solar PV window. In terms of maximum power generation, the RADTIRC-PV window generates 0.749 W at normal incidence, 4.8x higher than the non-concentrating counterpart.

**Keywords:** solar photovoltaic; solar concentrator; rotationally asymmetrical concentrator; building integrated photovoltaic system.

## 39 1. Introduction

40

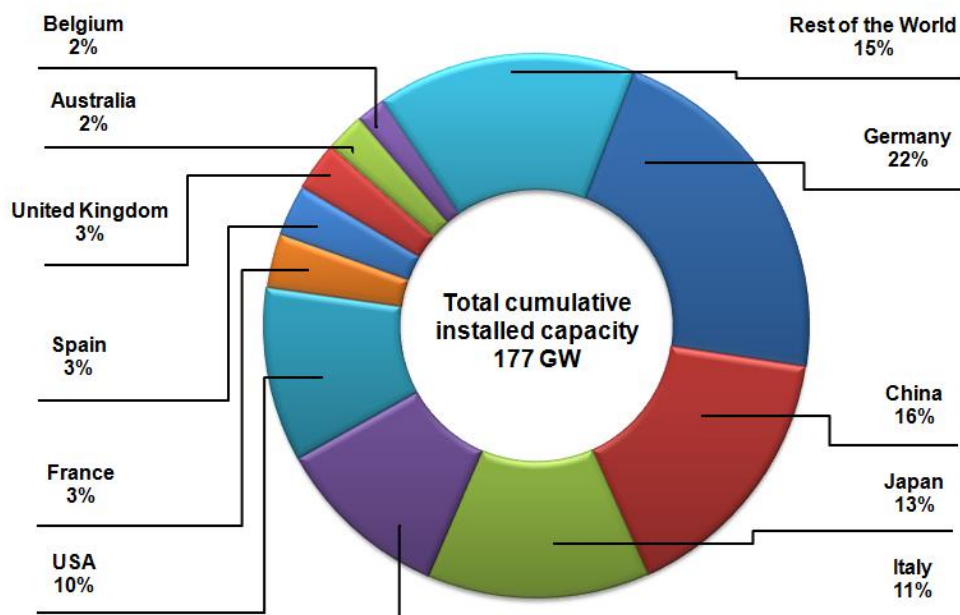
41 Solar photovoltaic (PV) – a technology that converts solar energy directly into  
42 electricity – has great potential in satisfying the world’s energy needs. The 2014 report [1]  
43 published by the International Energy Agency (IEA) emphasises that this technology will  
44 possibly be the “dominant power source by 2050”. Governments and private sectors have  
45 invested a huge amount of money on solar PV technology [2]. In 2014 alone, solar  
46 technology attracted approximately USD150 billion<sup>1</sup> (GBP94.5 billion)<sup>2</sup> worth of investment  
47 [2] for funding technology research, development, commercialisation, manufacturing and  
48 new projects. To further accelerate the uptake of solar PV, several governments have  
49 introduced a number of measures. One of the most effective ones is known as the feed-in  
50 tariff (FiT) scheme [3–7]. An FiT scheme pays a consumer a specific tariff per kWh of  
51 electricity generated from solar PV technology for a duration of time [8]. The FiT scheme has  
52 now been implemented in more than 80 countries [2]. The investment and policies have had a  
53 positive effect on solar PV installations worldwide with the cumulative installed capacity of  
54 177 GW by the end of 2014 [2]. From this figure, approximately 49% of these installations  
55 were carried out in Europe (see Fig. 1) [2]. It is reported that solar PV was considered as the  
56 fastest growing renewable technology in 2014 [2], with an average annual growth rate  
57 recorded at 30% when compared with the growth in 2013 [2]. To date, solar PV technology  
58 has created approximately 2.5 million jobs around the globe [2].

59

---

<sup>1</sup> Here, 1 billion is defined as 1 thousand million, i.e.  $10^9$ .

<sup>2</sup> Based on the conversion rate carried out on 10/11/2014, USD1.00 is equivalent to GBP0.63 [34]. This value is used throughout this paper.



60

61

Fig. 1: Cumulative PV installed capacity in 2014. Adapted from [2,9].

62

63 Despite the rapid growth in terms of installed capacity, solar PV only supplied around  
 64 1% of the world's electricity requirement in 2014 [9]. One of the reasons is the high capital  
 65 cost of installing a solar PV system, which ranges between USD1200 (GBP756) to  
 66 USD24000(GBP15120) per kWp according to the recent data from the IEA [10]. The largest  
 67 proportion of the cost is from the PV module (around 40%) [10], and the PV material  
 68 contributes up to 73% of the module cost [11], i.e. 29.2% of the overall installation cost. By  
 69 reducing the usage of PV material in a PV module, it is possible to achieve a cheaper PV  
 70 system which could further attract more consumers in opting for and installing this  
 71 technology.

72

73 One of the solutions suggested by several researchers to reduce the cost of a solar PV  
 74 module is to incorporate an optical concentrator into the solar PV design [12]. A concentrator  
 75 works by focusing the solar energy from a large entrance aperture area to a smaller exit  
 76 aperture area to which a solar PV cell is attached [12]. By doing this, the amount of PV  
 77 material can be reduced significantly while maintaining the same electrical output. The  
 78 concentrator can be fabricated using low cost materials such as plastic or mirrors, which  
 79 offsets the cost of the displaced PV material [12]. The PV technology that includes a low gain

80 concentrator (gains  $< 10x$ ) in the design is known as low-concentration photovoltaics  
81 (LCPV).

82 Researchers have proposed various designs of LCPV in the past 40 years. Pei *et al.*  
83 [13] demonstrated that a dielectric Compound Parabolic Concentrator (CPC) extrusion in an  
84 LCPV design was capable of increasing the electrical power by 73% when compared with the  
85 non-concentrating PV. Another study conducted by Goodman *et al.* [14] showed that a  
86 rotationally symmetrical dielectric CPC design increased the short circuit current of the  
87 LCPV system by a factor of 5.7x when compared with a bare solar cell. Muhammad-Sukki *et*  
88 *al.* [15] simulated the performance of an extrusion of a dielectric totally internally reflecting  
89 concentrator (DTIRC) and concluded that the design could increase the electrical output by  
90 nearly 5 times when compared with a non-concentrating system. From their analysis, their  
91 LCPV design could reduce the cost by 41% [16]. On the other hand, Sarmah *et al.* [17]  
92 showed that an LCPV design employing a dielectric extrusion of asymmetrical CPC  
93 produced 2.27 times more electrical power when compared with a system without a  
94 concentrator. Their LCPV design could reduce the cost of a solar panel by 20% per kWp  
95 [17]. Abu-Bakar *et al.* [18] proposed an LCPV system based on a rotationally asymmetrical  
96 CPC which could potentially increase the short circuit current by as much as 6.18 times than  
97 the non-concentrating counterpart.

98 This paper evaluates an LCPV design incorporating a novel concentrator known as  
99 the rotationally asymmetrical dielectric totally internally reflecting concentrator (RADTIRC).  
100 The authors has recently investigated a new RADTIRC prototype which was created from the  
101 polymethyl methacrylate acrylic (PMMA) material by using an injection moulding method  
102 and its performance was compared with the old prototype that was created from an acrylic  
103 type material known as '6091' by using a silicon moulding technique [19]. The study [19]  
104 concluded that the injection moulding technique enables the prototype to achieve a much  
105 closer dimension to the desired design than one created from silicon mould, with an area  
106 deviation of 0.8%. In terms of the selection of material, the concentrator created from PMMA  
107 material provides a much better performance than the '6091' material, an increase of 13.57%  
108 in terms of the short circuit current generated at normal incidence [19].

109 This paper aims to demonstrate that an LCPV system could be created (in this case a  
110 small solar PV window) by incorporating an array of 12 concentrators for use in building  
111 integration and at the same time could provide substantial electrical output when compared to  
112 a similar non-concentrating PV window. The electricity generated can be utilised in the

113 building, stored in a battery (for off-grid connection) or exported to the grid (for on-grid  
114 connection).

115

## 116 **2. System description**

117

### 118 2.1 Design of optical concentrator

119

120 The design of the optical concentrator discussed in this paper, for which there is a  
121 patent [20], is discussed in detail in [21]. The creation of the RADTIRC is complex where  
122 various 2D templates need to be created at each angle of rotation - with each template has the  
123 same total height but has different values of exit aperture width and half-acceptance angle.  
124 These two values (i.e. the exit aperture width and the half-acceptance angle) were  
125 predetermined by the programme from the input parameters chosen by the users. After 180 of  
126 these 2D templates are created, a point cloud is formed by combining all the surface point of  
127 these 2D templates to produce the desired RADTIRC. A variety of RADTIRC designs were  
128 simulated [21] and one specific design was fabricated and tested indoors and outdoors [22].  
129 The fabricated design has a total height of 3 cm, a square exit aperture of 1 cm by 1 cm, a  
130 geometrical concentration ratio<sup>3</sup> of 4.9069, an index of refraction of 1.5, two half-acceptance  
131 angles which are  $\pm 40^\circ$  along the x-axis and  $\pm 30^\circ$  along the z-axis (see Fig. 2) [22] to cater for  
132 variation of sun path during the day and throughout the year. Although the first prototype  
133 yielded a good result, two problems were identified: (i) the dimensions of the concentrator  
134 were smaller than the design specifications due to the usage of a silicon mould (see Fig. 3),  
135 and (ii) the material used in the prototype suffered a discoloration (from clear to yellowish  
136 colour as illustrated in Fig. 3) and photo degradation with time, which reduced its  
137 performance by 4% after 2 years. To overcome these problems, the same design was  
138 fabricated by UK Optical Plastic Limited using an injection moulding machine BOY 35M  
139 [23]. The material chosen for the concentrators is a variation of PMMA resin which is known  
140 as Altuglas® V825T and has a refractive index of 1.49 [24]. PMMA is a widely used material  
141 for optical concentrators due to its high transmittance (minimum 92%) and good resistance to  
142 photo degradation properties [25].

143

---

<sup>3</sup> For a 3D concentrator, a geometrical concentration ratio is defined as the area ratio of the area of the entrance aperture to the area of the exit aperture [35].

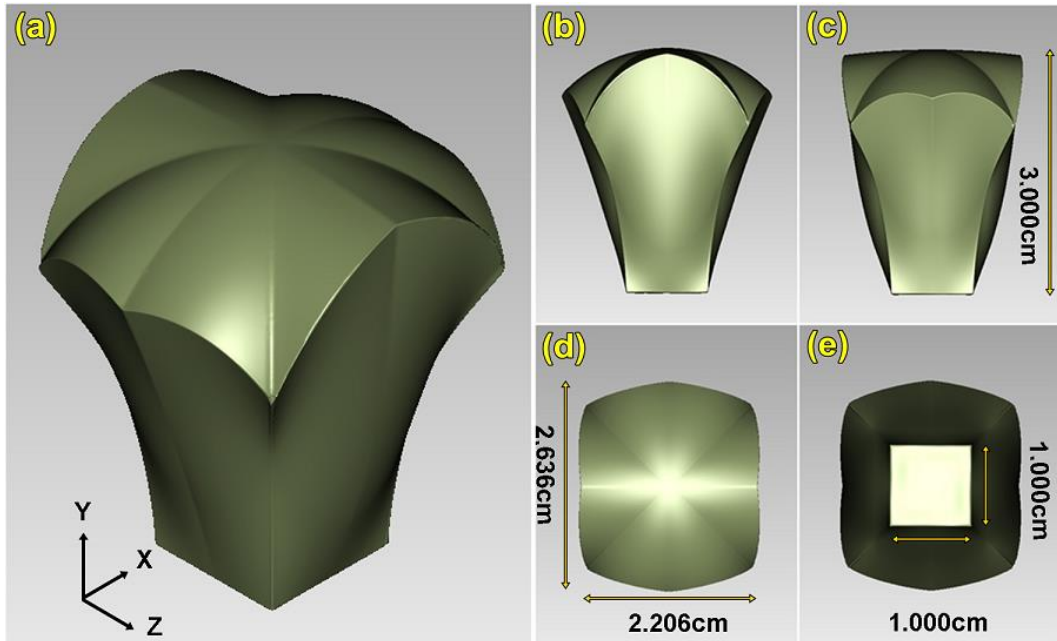


Fig. 2: Prototype RADTIRC dimensions.

144  
145  
146

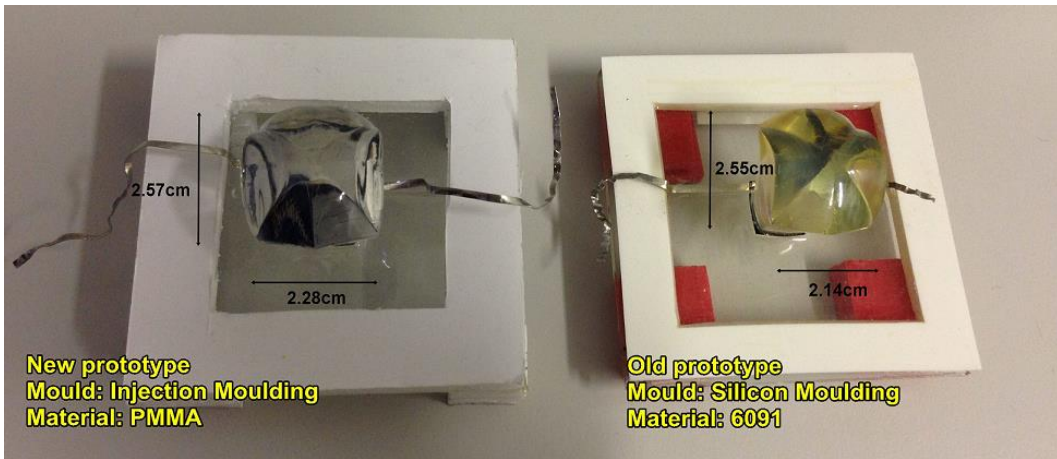


Fig. 3: Comparison of the old and new prototype of the RADTIRC.

147  
148  
149  
150  
151  
152  
153  
154  
155  
156  
157  
158

## 2.2 Solar cell

The solar cells used for the test were supplied by Solar Capture Technologies Ltd, United Kingdom and each cell has dimensions of 1 x 1 cm. These monocrystalline silicon solar cells have Laser Grooved Buried Contact (LGBC) and are suitable for LCPV applications [26].

## 2.3 Assembly process

159 The small solar PV window prototype <sup>4</sup> (250mm x 289mm x 70mm) was constructed  
160 by utilising 12 RADTIRC prototypes and 12 LGBC cells to create the concentrating-PV  
161 windows. The cells were interconnected in series using a pre-design template in a 4 x 3 array  
162 (see Fig. 4) and were then glued on a glass substrate. The arrangement of the cells was  
163 created in such a way that when the RADTIRCs were placed on the cells, these concentrators  
164 achieved the ‘best’ alignment between the cells and the exit aperture of the concentrators to  
165 minimise optical losses. The distance between two cell arrays was chosen such that the cells  
166 enabled the concentrators to create an optimum and compact arrangement of concentrators.  
167 i.e. the concentrators could be placed as close as possible to each other to create the ‘best’  
168 packaging density<sup>5</sup>. The RADTIRC here has a packaging density of 84%.

169 To permanently mount the concentrators on the solar cells, a silicon elastomer  
170 Sylgard-184® from Dow Corning was chosen as the binding material. This material also acts  
171 as an encapsulation material for the solar cells and as an index matching gel between the  
172 concentrator and the cells [22]. It has a high transmission value of 94.4% [27] and can be  
173 cured using a simple process [17,21,25]. The Sylgard-184® was prepared by mixing the  
174 supplied base and curing agent in a 10:1 weight ratio in a small beaker. The mixture is then  
175 placed in a vacuum chamber for 15 minutes to eliminate air bubbles. A Dow Corning Primer  
176 92-023 was applied on the solar cells for a better adhesion between the Sylgard and the cells.  
177 Once the Sylgard was free from air bubbles, the mixture was poured on top of the inter-  
178 connected cells. Afterwards, the RADTIRCs were placed carefully on top of the solar cells  
179 and the elastomer was left to cure for 48 hours under room temperature to ensure good  
180 binding between the concentrators and the cells. To compare the performance of this LCPV  
181 system with a non-concentrating one, a non-concentrating PV system was created using the  
182 same procedure and material.

183 Both the concentrating and non-concentrating PV systems were sent to Strathclyde  
184 Insulating Glass Limited, United Kingdom for assembly within sealed double glazing units  
185 and subsequently to Windowplus, United Kingdom to fabricate the window frames. The final  
186 form of the solar PV window incorporating the RADTIRCs is presented in Fig. 4.

---

<sup>4</sup> The length and the width of the window are chosen to fit bricks that are between 215mm and 300mm long according to an EU directive [36].

<sup>5</sup> Packaging density is defined as the percentage area of the entrance aperture of the concentrator in the entire module area [37]. For example, a square entrance aperture employs a higher packaging density (at 100%) when compared to a circular entrance aperture (at 79%).



Fig. 4: The solar PV window incorporating the RADTIRC design.

188

189

190

191

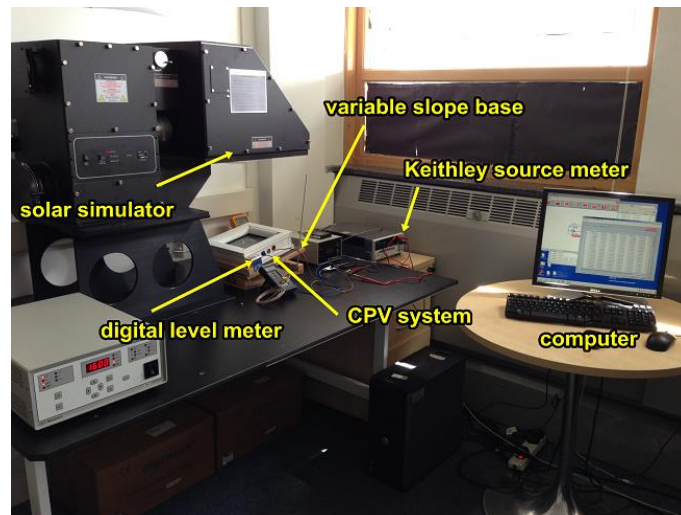
192

### 193 3. Experimental setup

194

195 The indoor experimental setup to evaluate the characteristic of the solar window  
196 incorporating the RADTIRC's is illustrated in Fig. 5. It follows the same setup to evaluate the  
197 singular RADTIRC-PV structure which was presented in [19]. A solar simulator (Class AAA,  
198 AM 1.5G irradiation spectrum), Oriel® Sol3A Model 94083A, from Newport Corporation  
199 was used to simulate direct solar radiation at the earth surface. A variable slope base was  
200 placed 38cm beneath the solar simulator's lamp and within the uniform illumination area  
201 (20cm x 20cm) of the lamp. A digital tilt meter was used to measure the tilt angle of the  
202 variable slope base. A Keithley 2440 source meter with 4-wire connections was utilised here  
203 to act as a loading circuit, but with more accuracy [22]. It was connected to a computer which  
204 was already installed with Lab Tracer software from National Instruments® to measure the  
205 electrical output from both solar windows.

206



207

208

Fig. 5: Indoor experimental setup.

209

#### 210 4. Results and discussions

211 When an array of the RADTIRC-PV cells is connected in series, in theory, the short  
212 circuit current generated from the array must be equal to the one generated from a single  
213 RADTIRC-PV structure studied previously by the authors in [19]. On the other hand, the  
214 maximum power and the open circuit voltage generated by the array will be increased by a  
215 factor of 12 since there are 12 RADTIRC-PV cells incorporated in the design. The  
216 information from the short circuit current is also needed to compare the opto-electronic gain  
217 of the concentrating-PV window with the one produced by the singular RADTIRC-PV  
218 structure. However, it is expected some losses will be introduced in the system causing the  
219 amount of the short circuit current and the opto-electronic gain produced by the RADTIRC-  
220 PV window to be lower than the ones produced by a single RADTIRC-PV structure. The  
221 value of the maximum output power (and the open circuit voltage) is also expected to be  
222 lower than the theoretically calculated i.e. lower than  $12 \times P_{max}$  (and  $V_{oc}$ ) generated from a  
223 single RADTIRC-PV structure.

224

##### 225 4.1 The characteristics of the RADTIRC-PV window

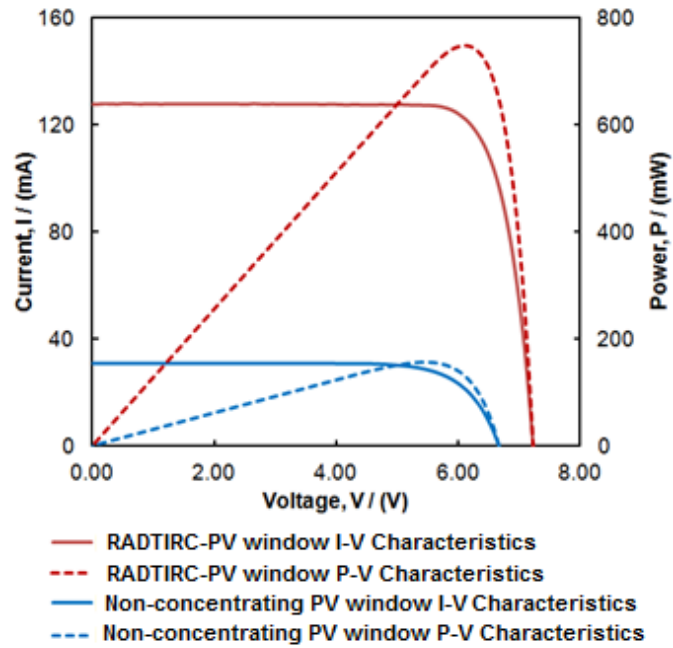
226

227 The RADTIRC-PV window was placed on the variable slope base. Under the  
228 standard test conditions, the solar simulator was configured to produce an irradiance of  
229  $1000\text{W/m}^2$  and the room temperature was set at  $25^\circ\text{C}$ . The door and windows of the room

230 were closed to avoid unwanted air flow and minimise temperature variation and the windows  
231 had blinds to prevent light from entering the room. The variable slope was set at  $0^\circ$ . For each  
232 measurement, the short circuit current ( $I_{sc}$ ), the open circuit voltage ( $V_{oc}$ ), the maximum  
233 current ( $I_{max}$ ), the maximum voltage ( $V_{max}$ ), the maximum power ( $P_{max}$ ) and the fill factor  
234 ( $FF$ ) were determined and recorded.

235 Fig. 6 shows the current-voltage (I-V) characteristics and the power-voltage (P-V)  
236 characteristics of the solar PV windows respectively. As it can be seen from Fig. 6, the short  
237 circuit current of the non-concentrating window was 0.031 A. However, the introduction of  
238 the RADTIRCs in the window increased the short circuit current by a factor of 4.13 when  
239 compared with the non-concentrating system, generating 0.128 A. As indicated earlier, the  
240 concentrator was concentrating the irradiance from the entrance aperture to the exit aperture.  
241 This increased the intensity of the light that impinged on the RADTIRC-PV window linearly  
242 [28], resulting in a higher short circuit current than the one produced from the non-  
243 concentrating window. The open circuit voltage was also increased from 6.65 V to 7.20 V  
244 when the RADTIRC-PV window was compared with a non-concentrating PV window.  
245 Unlike the short circuit current, the open circuit voltage increased logarithmically with  
246 irradiance concentration [28]. The maximum power on the other hand was increased from  
247 0.156 W to 0.749 W when the RADTIRC-PV window was compared with the non-  
248 concentrating PV window, giving a maximum power ratio of 4.8. The experiment showed  
249 that the RADTIRC-PV window increased the fill factor from 76% to 81% mainly due to an  
250 increase in both the short circuit current and the open circuit voltage of the concentrator. In  
251 terms of electrical conversion efficiency, the introduction of concentrators in the solar  
252 window reduced this value from 13% to 12.72%.

253



254

255 Fig. 6: Electrical outputs from the solar PV windows under standard test conditions.

256

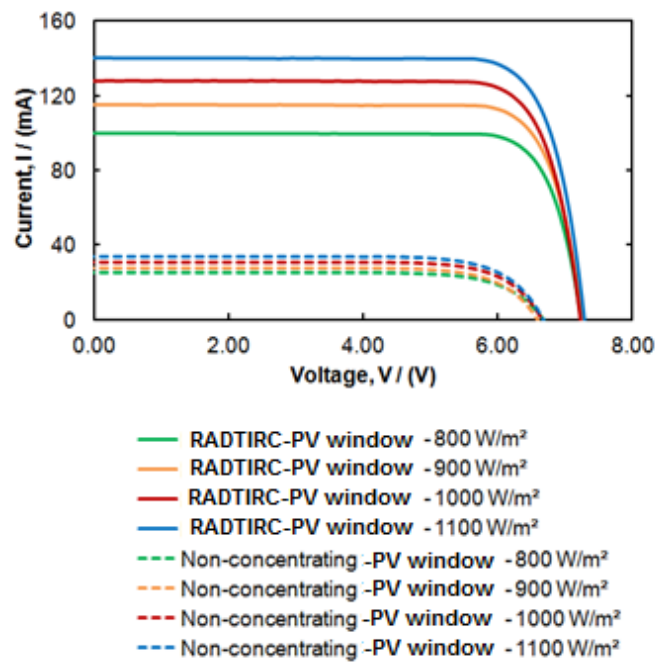
257 The output from the RADTIRC-PV window is compared with the result obtained  
 258 from a single RADTIRC-PV structure studied in [19]. The short circuit current generated  
 259 from the RADTIRC-PV window decreased to 0.128 A from 0.159 A when compared to the  
 260 one produced by a single RADTIRC-PV structure, a reduction of 19.4%. The maximum  
 261 power on the other hand increased by a factor of 9.9 instead of a factor of 12, generating a  
 262 maximum power value of 75.9 W. As for the non-concentrating PV window, its short circuit  
 263 current reduced to 0.030 A from 0.036 A when compared to the one produced by a single PV  
 264 cell, a reduction of 16.7%. In terms of the maximum power generated, the non-concentrating  
 265 PV window increased this value by 10.1 when compared to amount produced by a single bare  
 266 cell, achieving a maximum power value of 0.156 W. This losses could be attributed to many  
 267 factors, including (i) manufacturing errors causing the dimensions of the concentrator to  
 268 differ from the actual design dimensions, uneven surfaces of the entrance aperture and over  
 269 polishing on the profile of the side wall; (ii) assembly errors during the soldering of the  
 270 tabbing wire on the solar cells which reduced the effective area of each cell, misalignment  
 271 between the solar cells and the exit aperture of the concentrators, misalignment on the  
 272 arrangement in the arrays of the concentrators along the x and z-axes and losses due to the  
 273 index matching gel at the lower part of the concentrator profile, and (iii) errors associated

274 with the rays such as scattering reflection on the front surface of the concentrator which  
275 reduces the number of rays reaching the exit aperture of the RADTIRC.

276

277 It is also useful to see the variation of I-V and P-V- characteristics under various level  
278 of solar radiation. The experiment was repeated by varying the output from the solar  
279 simulator between  $800\text{W/m}^2$  and  $1100\text{W/m}^2$  and the results are presented in Figs. 7 and 8.  
280 When the intensity of the sun simulator increased from  $800\text{W/m}^2$  to  $1100\text{W/m}^2$ , the short  
281 circuit current from both solar windows increased - from  $0.100\text{A}$  to  $0.140\text{A}$  for the  
282 RADTIRC-PV window and from  $0.025\text{A}$  to  $0.034\text{A}$  for the non-concentrating PV window. In  
283 terms of the maximum power, the change in simulator's intensities caused the reading from  
284 the panels to rise from  $0.593\text{W}$  to  $0.825\text{W}$  and from  $0.125\text{W}$  to  $0.170\text{W}$  for the RADTIRC-  
285 PV window and the non-concentrating PV window respectively.

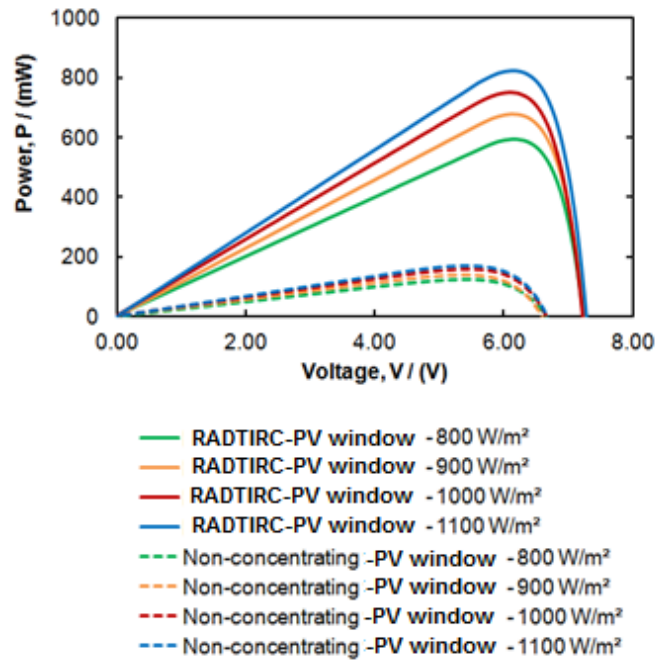
286



287

288 Fig. 7: The I-V characteristics of the solar PV windows under various levels of irradiance.

289



290

291 Fig. 8: The P-V characteristics of the solar PV windows under various levels of irradiance.

292

#### 293 4.2 The angular response of the RADTIRC-PV window

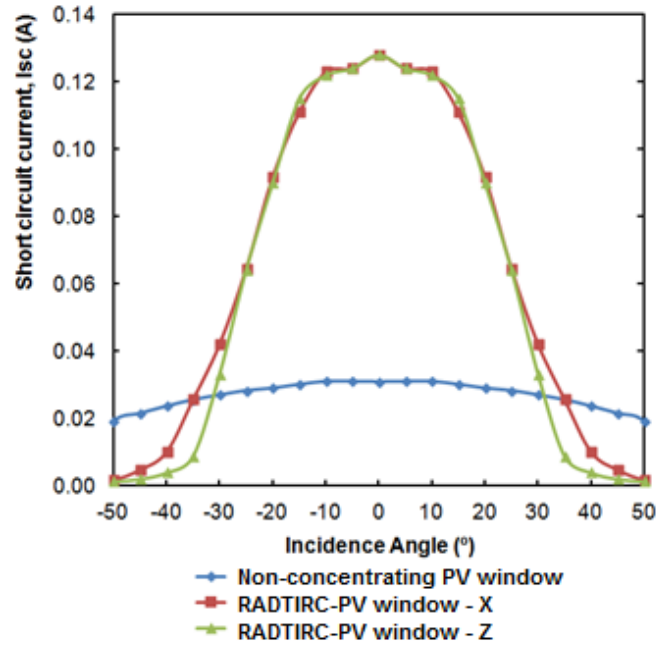
294

295 The next part of the experiment consisted in characterising the angular response of the  
 296 RADTIRC-PV window. This was carried out by setting the output of the solar simulator at  
 297  $1000\text{W/m}^2$  and setting the room temperature at  $25^\circ\text{C}$ . The variable slope base was tilted from  
 298  $0^\circ$  to  $50^\circ$  at increments of  $5^\circ$ , with each tilt angle measured using the digital level meter. For  
 299 each angular increment, the short circuit current ( $I_{sc}$ ), the open circuit voltage ( $V_{oc}$ ), the  
 300 maximum current ( $I_{max}$ ), the maximum voltage ( $V_{max}$ ), the maximum power ( $P_{max}$ ) and the fill  
 301 factor ( $FF$ ) were determined and recorded.

302 The variation of the short circuit current is presented in Fig. 9 and the maximum  
 303 output power of the windows is presented in Fig. 10, both plotted against the incidence angle.  
 304 In general, both parameters decreased gradually when the angle of incidence increased. From  
 305 Fig. 9, it was found that the RADTIRC-PV window achieved its maximum short circuit  
 306 current at normal incidence, with the value of  $0.128\text{A}$  recorded. The RADTIRC-PV window  
 307 achieved 90% of its peak short circuit value when the angle of incidence was at  $\pm 15^\circ$  along  
 308 the x-axis and at  $\pm 14^\circ$  along the z-axis. This value reduced to half when the angle of  
 309 incidence of the rays reached  $\pm 25^\circ$ . When the angle of incidence was equal to the minimum  
 310 ‘design’ half-acceptance angle (along the z-axis), the maximum current was always higher

311 than the one generated from the non-concentrating PV solar window, as illustrated in Fig. 9.  
312 Beyond this angle of incidence, the short circuit current continued to decrease eventually  
313 reaching a value of 0A.

314



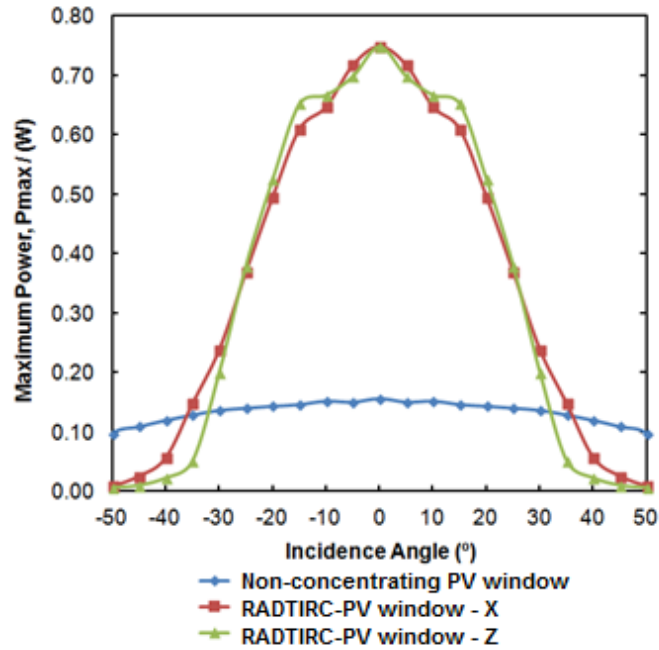
315

316 Fig. 9: The short circuit current of the solar PV windows at different angles of incidence.

317

318 In terms of maximum output power, the variation of maximum output power against  
319 the incidence angle is presented in Fig. 10. When compared with the short circuit current, a  
320 similar trend was observed for the values of maximum output power. The peak value of  
321 maximum output power was achieved at normal incidence, with the value of 0.749W  
322 recorded. The RADTIRC-PV window achieved 90% of its peak short circuit value when the  
323 angle of incidence was at  $\pm 15^\circ$  along the x-axis and at  $\pm 14^\circ$  along the z-axis. This value  
324 decreased to half when the angle of incidence of the rays reached  $\pm 26^\circ$ . When the angle of  
325 incidence was equal to the minimum 'design' half-acceptance angle (along the z-axis), the  
326 maximum power was always higher than the one produced from the non-concentrating PV  
327 window, as indicated in Fig. 10. Beyond this angle of incidence, the maximum power  
328 continued to decrease until it reached a value of 0W.

329



330

331 Fig. 10: The maximum power of the solar PV windows at different angles of incidence.

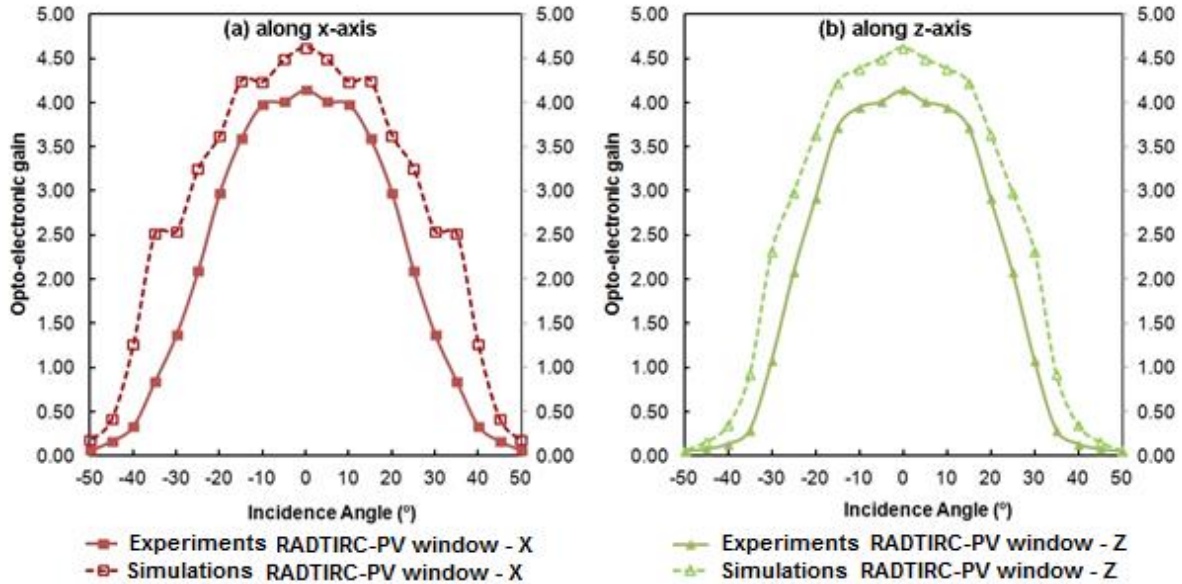
332

333 The opto-electronic gain of the concentrator was also plotted against the incidence  
 334 angle and it is presented in Fig. 11. The opto-electronic gain measures the ratio of short  
 335 circuit current produced from an LCPV system to the one generated from a conventional non-  
 336 concentrating one [17,22,29]. The maximum opto-electronic gain was obtained at normal  
 337 incidence, with a value of 4.13, achieving an optical efficiency of 84%. The RADTIRC-PV  
 338 window achieved 90% of its peak opto-electronic gain value when the angle of incidence was  
 339 at  $\pm 15^\circ$  along the x-axis and at  $\pm 14^\circ$  along the z-axis. This value reduced to half when the  
 340 angle of incidence of the rays reached  $\pm 25^\circ$ . When the angle of incidence was equal to the  
 341 minimum ‘design’ half-acceptance angle (along the z-axis), the gain was always higher than  
 342 1, as indicated in Fig. 11. Outside this incidence angle, the opto-electronic gain dropped  
 343 gradually to 0.

344 The opto-electronic gains are compared with the optical gains from the simulations  
 345 (see Fig. 11). The simulations were carried out using an optical software ZEMAX® and the  
 346 detail simulation steps have been presented in [21]. The results from the experiment show  
 347 good agreement with the simulation data, with a deviation of 10% at the peak value. This  
 348 deviation can be contributed to several factors, which include (i) manufacturing errors  
 349 causing the dimensions of the concentrator to differ from the actual design dimensions,  
 350 uneven surfaces of the entrance aperture and over polishing on the profile of the side wall,

351 and (ii) assembly errors during the soldering of the tabbing wire on the solar cells which  
 352 reduced the effective area of each cell, misalignment between the solar cells and the exit  
 353 aperture of the concentrators and misalignment on the arrangement in the arrays of the  
 354 concentrators along the x and z-axes.

355



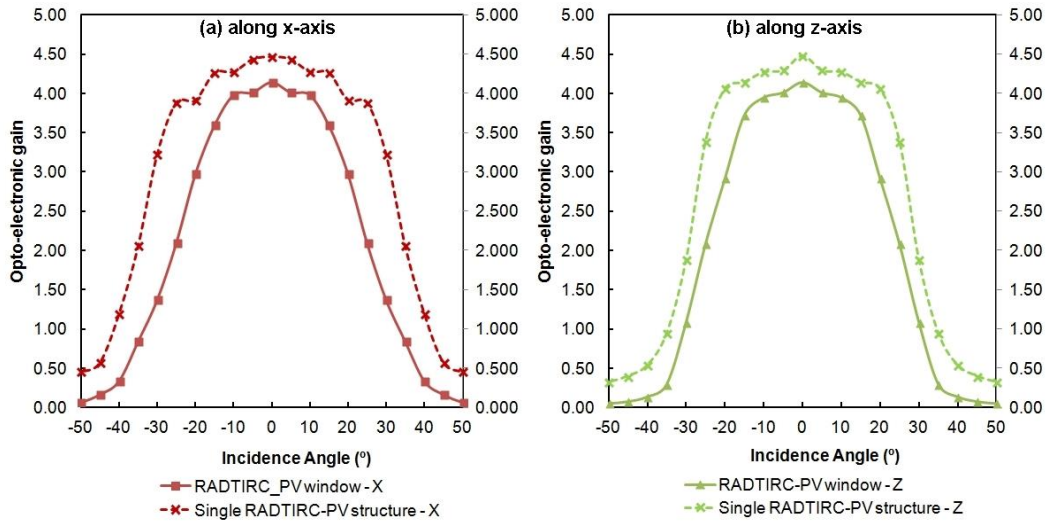
356

357 Fig. 11: The optical gain of the RADTIRC-PV window.

358

359 The opto-electronic gain generated from the RADTIRC- PV window is also compared  
 360 to the one produced by a single RADTIRC-PV structure [19], and the results are presented in  
 361 Figure 12. As expected, the value of the opto-electronic gain of the RADTIRC-PV window is  
 362 always lower than the one produced by a single RADTIRC-PV structure at all angles of  
 363 incidence, with a deviation of 7.8% at normal incidence due to losses attributed to several  
 364 factors described earlier in Section 3.8.1

365

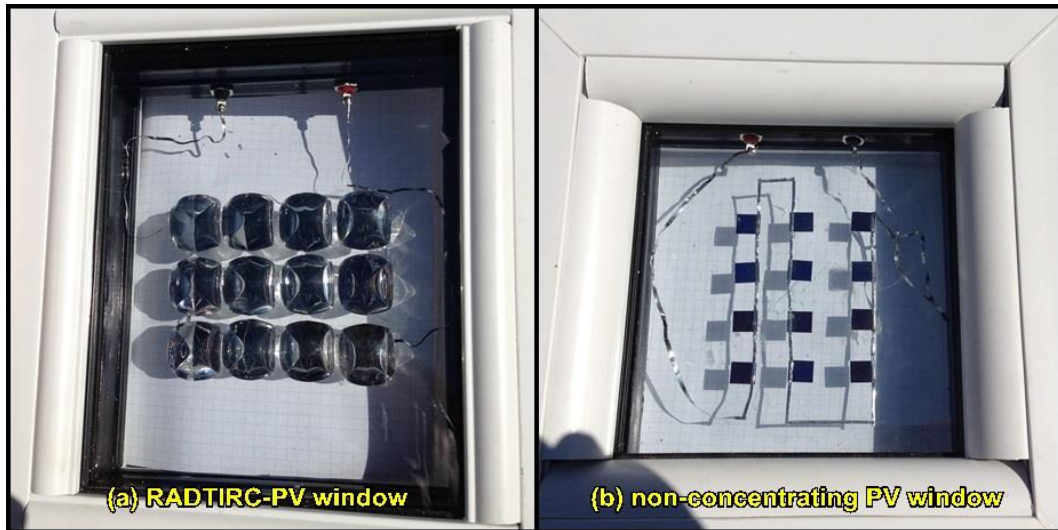


366

367 Fig. 12: Comparison of the opto-electronic gain generated from the RADTIRC-PV window  
 368 and a single RADTIRC-PV structure.

369

370 It is also interesting to see that the opto-electronic gain has a large drop when the  
 371 angle of incidence of the rays was  $\pm 20^\circ$  and wider. This was because parts of the RADTIRCs  
 372 were shaded by the frame of the window (see Figure 13(a)) which reduced the amount of  
 373 short circuit current from the RADTIRC-PV window. The non-concentrating window  
 374 experienced the same effect when the angle of incidence of the rays was larger than  $\pm 35^\circ$ .  
 375 The largest deviation between the reading of the RADTIRC-PV window and the single  
 376 RADTIRC-PV structure occurred when the angle of incidence of the rays was at  $\pm 30^\circ$  when  
 377 half of the RADTIRCs were shaded, giving a deviation of 58%. There was no shadowing  
 378 occurring in the single RADTIRC-PV structure tested in [19] since it was frameless. It is  
 379 therefore important to ensure that the arrays of the concentrators and the PV cells are  
 380 integrated in such a way that the shadowing of the cells is avoided in order to maximise the  
 381 generation of electrical output from the LCPV systems.



382

383

Fig. 13: Shadowing effect on the solar PV windows.

384

385

386

387 4.3 The effect of temperature on the maximum power generated by the RADTIRC-PV  
388 window

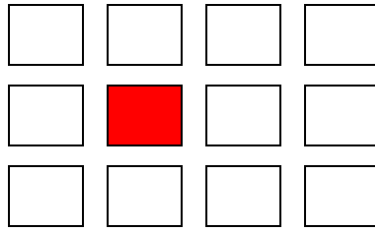
389

390 This section evaluates the effect of temperature on the performance of the RADTIRC-  
391 PV window. For this purpose, two thermocouples were utilised; one was attached at the back  
392 of the glass panel beneath one of the solar cells<sup>6</sup> (see Fig. 14), and another one was used to  
393 measure the room temperature. The RADTIRC-PV window was placed at 0° inclination. The  
394 solar simulator was configured to produce 1000 W/m<sup>2</sup> and the room temperature was set at  
395 25°C. The RADTIRC-PV window was exposed to the same radiation for a period of 4.5  
396 hour. A set of readings was taken at intervals of 15 minutes.

397

---

<sup>6</sup> The most accurate way of measuring the temperature would be to place the thermocouple exactly beneath the solar cell. However, based on the heat transfer model using the ANSYS 12.1 software developed by Kumar et al. [38] and Sellami [39] to compare the temperature at the back of the solar cell and at the back of the glass substrate, it was demonstrated that the temperature reading at both location via simulation matched the experimental data accurately. Therefore, this setup is used in this study.



398

399

400

Fig. 14: The top view of the location of the thermocouple (marked in red) attached underneath one of the cells of the RADTIRC-PV window.

401

402

403

404

405

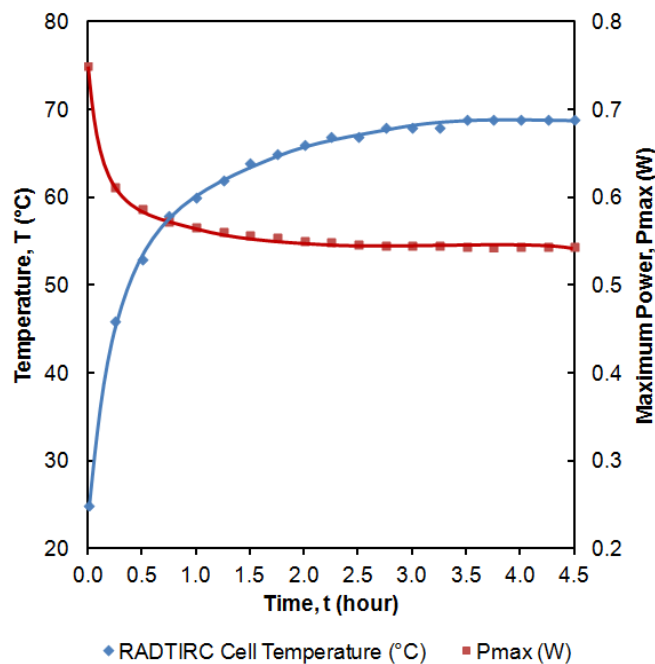
406

407

408

409

Fig. 15 shows the effect of temperature on the maximum power of the RADTIRC-PV window. The temperature of the cell increased sharply from 25°C to 69°C and stabilised after 3 hours. The maximum power reduced from 0.75W to 0.54W, a reduction of 27%. Table 1 presented the variations of the main parameters throughout the duration of the experiment. It was observed that the maximum current showed a slight reduction, from 0.12A to 0.10A. The maximum voltage however showed a considerable fall from 6.12 V to 5.20 V. As for the fill factor, the value reduced from 81% to 79%.



410

411

412

Fig. 15: Variation of RADTIRC-PV cell maximum power and temperature with illumination time.

413

414

Table 1: Effect of temperature on the RADTIRC-PV window output.

Time	Room	CPV	$V_{max}$	$I_{max}$	$P_{max}$	$V_{oc}$	$I_{sc}$	FF
	Temperatur	Temperatur						
	e	e						
(hour)	(°C)	(°C)	(V)	(A)	(W)	(V)	(A)	
0.00	25	25	6.12	0.12	0.75	7.20	0.13	0.81
0.25	29	46	5.71	0.11	0.61	6.85	0.11	0.80
0.50	30	53	5.51	0.11	0.59	6.65	0.11	0.79
0.75	31	58	5.51	0.10	0.57	6.55	0.11	0.79
1.00	32	60	5.41	0.10	0.57	6.50	0.11	0.78
1.25	32	62	5.31	0.11	0.56	6.45	0.11	0.78
1.50	33	64	5.31	0.10	0.56	6.40	0.11	0.78
1.75	33	65	5.31	0.10	0.55	6.35	0.11	0.79
2.00	33	66	5.20	0.11	0.55	6.35	0.11	0.78
2.25	33	67	5.31	0.10	0.55	6.30	0.11	0.78
2.50	33	67	5.20	0.10	0.55	6.30	0.11	0.78
2.75	33	68	5.20	0.10	0.55	6.30	0.11	0.78
3.00	33	68	5.20	0.10	0.54	6.30	0.11	0.78
3.25	33	68	5.20	0.10	0.54	6.30	0.11	0.78
3.50	33	69	5.20	0.10	0.54	6.25	0.11	0.79
3.75	33	69	5.21	0.10	0.54	6.25	0.11	0.79
4.00	33	69	5.20	0.10	0.54	6.25	0.11	0.79
4.25	33	69	5.20	0.10	0.54	6.25	0.11	0.79
4.50	33	69	5.20	0.10	0.54	6.25	0.11	0.79

416

417

418

419 It is also useful to identify the temperature coefficient for maximum current,  
420 maximum voltage and maximum power, which are obtained by calculating the ratio of  
421 change in each parameter with respect to the change in temperature [22,30]. It was calculated  
422 that the maximum voltage coefficient was  $0.021V/^\circ C$ , the maximum current coefficient was  
423  $0.454mA/^\circ C$  and the maximum power coefficient was  $0.005W/^\circ C$ .

424

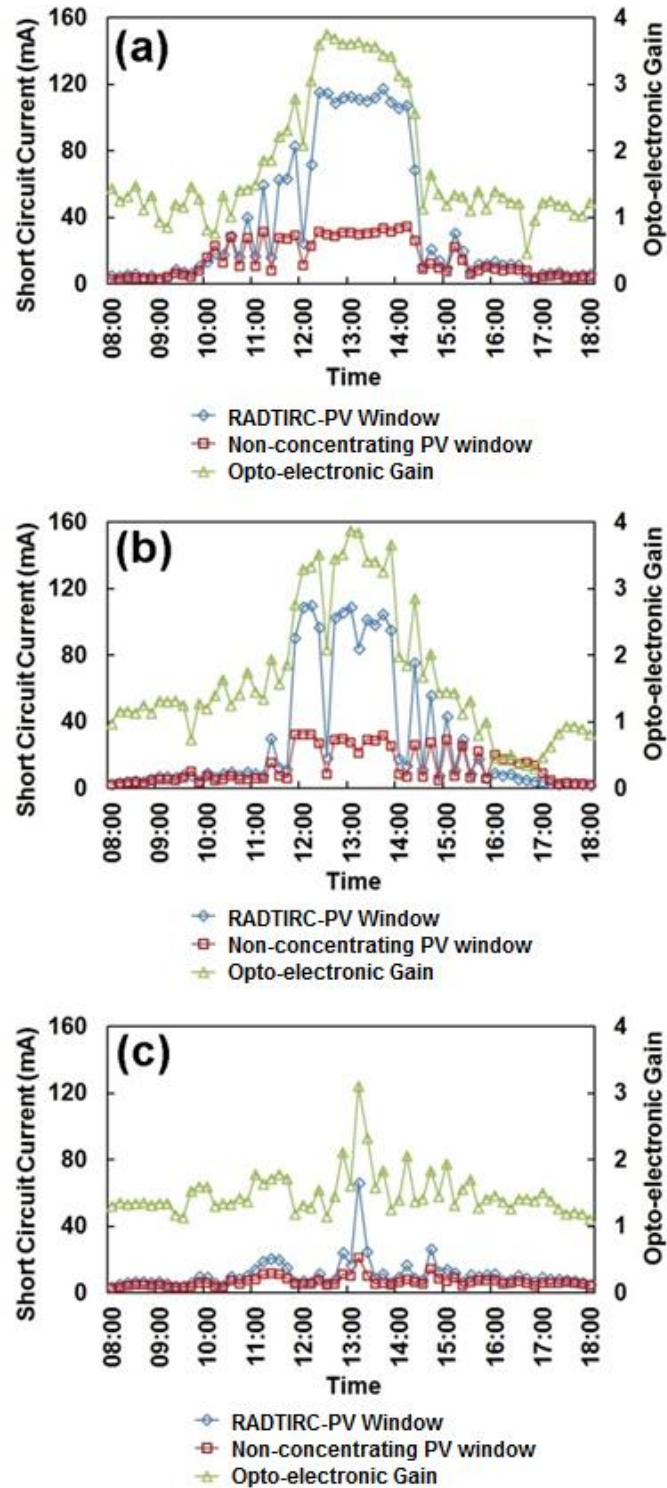
## 425 **5.0 The outdoor experiments**

426

427 Solar radiation consists of direct and diffuse radiation [31], and each one has a  
428 different effect on the performance of the solar PV windows. The outdoor performance of the  
429 panels in an open environment has also been investigated. During a sunny day, most of the  
430 radiation is direct, but on completely cloudy days, the radiation is mostly diffuse [31]. The  
431 outdoor experiments were conducted in Coventry Drive, Glasgow (55.865659°N,  
432 4.21063°W) between 20 June 2014 and 01 July 2014. Both panels were facing true south,  
433 (taking into account the magnetic declination of 3.35°W) and were tilted 33° from the  
434 horizontal to ensure 0° inclination with respect to the sun elevation angle. The information  
435 about the daily sun path and its elevation angle were obtained from [32]. A multimeter was  
436 connected to each panel to get simultaneous readings which measure the short circuit current  
437 produced by the panels. Simultaneous readings from the multimeters were taken at intervals  
438 of 10 minutes for a duration of 10 hours, i.e. from 8.00am until 6.00pm each day.

439 Fig. 16 shows selected results obtained from the experiment. In general, the  
440 introduction of the RADTIRCs increased the short circuit current generated from the panel.  
441 Based on the theory and the indoor experiments, the RADTIRC-PV window should produce  
442 much higher short circuit current than the non-concentrating system within its ‘design’  
443 acceptance angle under direct radiation. Based on the sun path information [32], the higher  
444 capture time should occur between 11.30am and 2.30pm. This trend can be observed during  
445 almost every sunny day (see Fig. 16(a)), where the RADTIRC-PV window generated a much  
446 higher short circuit current than the non-concentrated one, which confirms both the theory  
447 and the indoor experiments. The maximum short circuit current reading recorded was  
448 114.3mA, much higher than the 30.35mA generated from the non-concentrating PV window.  
449 This corresponded to the maximum opto-electronic gain value of 3.77. A similar trend was  
450 also observed in a partially sunny day, as illustrated in Fig. 14(b), with the maximum short  
451 circuit current generated from the RADTIRC-PV window and non-concentrating PV window  
452 being 109.2mA and 28.09mA respectively, providing an opto-electronic gain of 3.89.

453



454

455 Fig. 16: Results from outdoor experiments;(a) during an almost clear sky day; (b) during a  
 456 partially clear sky day, and (c) during a cloudy day.

457

458 It is interesting to observe the performance of both panels during a cloudy day, and  
 459 the example is presented in Fig. 14(c). It was observed that the RADTIRC-PV window

460 performed slightly better than the non-concentrating counterpart throughout the cloudy day,  
461 giving an opto-electronic gain value of minimum 1.1 for the whole period of 10 hours. This  
462 indicates that outside the ‘design’ half-acceptance angles of the concentrator, the diffuse  
463 radiation is still collected from the entrance aperture as well as the side profile of the  
464 concentrator to reach the solar cells, hence increasing the short circuit current generated from  
465 the solar windows.

466 From the observations during sunny and cloudy days, it is possible to conclude that  
467 the RADTIRC is capable to increase the short circuit current generated from the window. It is  
468 argued that the panel could not achieve its peak opto-electronic gain due to some factors.  
469 These include misalignment of the panels with reference to the sun path, errors in positioning  
470 the panel to face the true south, the frequently varying solar insolation, the formation of  
471 clouds, as well as changes in wind speed which caused the gain to reduce significantly.

472

## 473 **Conclusions**

474

475 A new type of solar window incorporating a novel RADTIRC design was proposed  
476 for BIPV system. The steps to assemble a RADTIRC-PV cells array within a double glazed  
477 window have been explained in detail. This panel underwent a series of analysis both indoors  
478 and outdoors and these results were compared with a non-concentrating panel. From the  
479 indoor experiments, it was found that the introduction of the RADTIRCs in the window could  
480 increase the short circuit current by a factor of 4.13 when compared with the non-  
481 concentrating PV system, generating 0.128 A. The maximum power on the other hand was  
482 increased from 0.156 W to 0.749 W when the RADTIRC-PV window was compared with the  
483 non-concentrating PV window, giving a maximum power ratio of 4.8. The output from the  
484 RADTIRC-PV window was also compared with the result obtained from a single RADTIRC-  
485 PV structure studied previously by the author in [19]. The short circuit current generated  
486 from the RADTIRC-PV window decreased to 0.128 A from 0.159 A when compared to the  
487 one produced by a single RADTIRC-PV structure, a reduction of 19.4%. The maximum  
488 power on the other hand increased by a factor of 9.9 instead of a factor of 12, generating a  
489 maximum power value of 75.9. As for the non-concentrating PV window, its short circuit  
490 current reduced to 0.030 A from 0.036 A when compared to the one produced by a single PV  
491 cell, a reduction of 16.7%. In terms of the maximum power generated, the non-concentrating  
492 PV window increased this value by 10.1 when compared to the amount produced by a single  
493 bare cell, achieving a maximum power value of 0.156 W. These losses could be attributed to

494 many factors, including manufacturing errors, assembly errors and errors associated with the  
495 rays which reduce the number of rays reaching the exit aperture of the RADTIRC.

496 In terms of the opto-electronic gain, it was also found that within the minimum  
497 'design' half-acceptance angle of the RADTIRC, the opto-electronic gain of the RADTIRC-  
498 PV window was always higher than 1, with a maximum value of 4.13x. The opto-electronic  
499 gain was also compared with the simulation and the results from the experiment showed good  
500 agreement with the ZEMAX® simulations. The opto-electronic gain generated from the  
501 RADTIRC- PV window was also compared to the one produced by a single RADTIRC-PV  
502 structure. As expected, the value of the opto-electronic gain of the RADTIRC-PV window  
503 was always lower than the one produced by a single RADTIRC-PV structure at all angles of  
504 incidence, with a deviation of 7.8% at normal incidence due to losses attributed to several  
505 factors described earlier in the previous paragraph, as well as due to shading from the frame  
506 of the windows. In terms of effect of the temperature on the performance of the RADTIRC-  
507 PV window, it was demonstrated that the maximum steady state temperature of the panel for  
508 the experimental setup used was 69°C, achieved within 3 hours of exposure to the sun. The  
509 corresponding maximum power during the steady state was recorded at 0.54W. The  
510 maximum voltage coefficient, the maximum current coefficient and the maximum power  
511 coefficient were determined to be 0.021V/°C, 0.454mA/°C and 0.005W/°C. As for the  
512 outdoor experiments, the variations of short circuit current and opto-electronic gain were  
513 plotted for a duration of 10 hours for several days. Under direct radiation, the RADTIRC-PV  
514 window generated a maximum opto-electronic gain of 3.89 while under diffuse radiation, the  
515 opto-electronic gain varied with a minimum value of 1.1.

516 It can be concluded that the RADTIRC has the potential to increase the electrical  
517 output from a solar window. Within the half-acceptance angle of the RADTIRC, the short  
518 circuit current and the maximum power are always higher than the ones generated from non-  
519 concentrating PV window. Despite this advantage, a longer exposure to the sun could  
520 increase the temperature of the cells in the window, which will reduce the maximum power  
521 of the RADTIRC-PV window - in this paper by 27%. It is therefore desirable to reduce the  
522 temperature of the cells to ensure a maximum output from the RADTIRC-PV window. This  
523 can be achieved by introducing a hybrid/thermal system using air that utilises the co-  
524 generated heat to stimulate ventilation in the building [15,21,33].

525

526 This paper demonstrated that an LCPV structure (in this case a solar PV window)  
527 could be constructed for use in a BIPV system. The LCPV design could also provides  
528 substantial gain in the electrical output when compared to a non-concentrating PV design.  
529 However, careful consideration is required to minimise the losses in the system.

530 Some of the future work that could be investigated include (i) detailed analysis on the  
531 effect of diffuse radiation on the windows' performance; (ii) long term evaluation of the  
532 windows outdoors, (iii) prediction of electrical output for a particular location based on  
533 meteorological data, and (iv) analysis of PV window incorporating a different variation of  
534 RADTIRC which could produce more energy specifically for vertical integration in a  
535 building.

536

### 537 **Acknowledgments**

538

539 This project is funded by Glasgow Caledonian University (GCU), Scotland's Energy  
540 Technology Partnership (ETP) and Majlis Amanah Rakyat (MARA), Malaysia. The authors  
541 would like to acknowledge the collaboration of AES Ltd. and its contribution to this project.  
542 Thanks are due to Mr Ian Baistow from Solar Capture Technologies Ltd, United Kingdom for  
543 providing the solar cells, Mr Antoine Y Messiou from UK Optical Plastics Limited, United  
544 Kingdom for fabricating the concentrators, Mr Mark Kragh from Off- Grid Europe, Germany  
545 for supplying the tabbing wire, Mr Martin Blore from Strathclyde Insulating Glass Limited,  
546 United Kingdom for creating the sealed double glazing unit, Mr Robert Tierney from  
547 Windowplus, United Kingdom for fabricating the window frame and Mr Robert Adamson  
548 from Glasgow Caledonian University, United Kingdom for creating the connections in the  
549 solar window panels.

550

### 551 **References**

552 [1] IEA. Energy Technology Perspectives 2014: Executive Summary. 2014.

553 [2] REN21. Renewables 2015 Global Status Report. France: 2015.

554 [3] Ahmad S, Tahar RM, Muhammad-Sukki F, Munir AB, Rahim RA. Role of feed-in tariff  
555 policy in promoting solar photovoltaic investments in Malaysia: A system dynamics approach.  
556 Energy 2015;84:808–15.

- 557 [4] Gallego-Castillo C, Victoria M. Cost-free feed-in tariffs for renewable energy deployment in  
558 Spain. *Renewable Energy* 2015;81:411–20.
- 559 [5] Huenteler J. International support for feed-in tariffs in developing countries—A review and  
560 analysis of proposed mechanisms. *Renewable and Sustainable Energy Reviews* 2014;39:857–  
561 73.
- 562 [6] Tsai W-T. Feed-in tariff promotion and innovative measures for renewable electricity: Taiwan  
563 case analysis. *Renewable and Sustainable Energy Reviews* 2014;40:1126–32.
- 564 [7] Campoccia A, Dusonchet L, Telaretti E, Zizzo G. An analysis of feed-in tariffs for solar PV in  
565 six representative countries of the European Union. *Solar Energy* 2014;107:530–42.
- 566 [8] Muhammad-Sukki F, Munir AB, Ramirez-Iniguez R, Abu-Bakar SH, Mohd Yasin SH,  
567 McMeekin SG, et al. Solar photovoltaic in Malaysia: The way forward. *Renewable and*  
568 *Sustainable Energy Reviews* 2012;16:5232–44.
- 569 [9] IEA-PVPS. 2014 Snapshot of Global PV Markets. 2015.
- 570 [10] IEA-PVPS. Trends 2015 in Photovoltaic Applications. 2015.
- 571 [11] Goodrich A, Hacke P, Wang Q, Sopori B, Margolis R, James TL, et al. A wafer-based  
572 monocrystalline silicon photovoltaics road map: Utilizing known technology improvement  
573 opportunities for further reductions in manufacturing costs. *Solar Energy Materials and Solar*  
574 *Cells* 2013;114:110–35.
- 575 [12] Muhammad-Sukki F, Ramirez-iniguez R, Mcmeekin SG, Stewart BG, Clive B. Solar  
576 Concentrators. *International Journal of Applied Sciences* 2010;1:1–15.
- 577 [13] Pei G, Li G, Su Y, Ji J, Riffat S, Zheng H. Preliminary Ray Tracing and Experimental Study  
578 on the Effect of Mirror Coating on the Optical Efficiency of a Solid Dielectric Compound  
579 Parabolic Concentrator. *Energies* 2012;5:3627–39.
- 580 [14] Goodman NB, Ignatius R, Wharton L, Winston R. Solid-dielectric compound parabolic  
581 concentrators: on their use with photovoltaic devices. *Applied Optics* 1976;15:2434–6.
- 582 [15] Muhammad-Sukki F, Ramirez-Iniguez R, McMeekin S, Stewart B, Clive B. Optimised  
583 Dielectric Totally Internally Reflecting Concentrator for the Solar Photonic Optoelectronic  
584 Transformer System: Maximum Concentration Method. In: Setchi R, Jordanov I, Howlett R,  
585 Jain L, editors. *Knowledge-Based and Intelligent Information and Engineering Systems SE -*  
586 *67*, vol. 6279, Springer Berlin Heidelberg; 2010, p. 633–41.
- 587 [16] Muhammad-Sukki F, Ramirez-Iniguez R, McMeekin SG, Stewart BG, Clive B. Optimisation  
588 of Concentrator in the Solar Photonic Optoelectronic Transformer : Comparison of  
589 Geometrical Performance and Cost of Implementation. *International Conference on*  
590 *Renewable Energies and Power Quality (ICREPPQ'11)*, Las Palmas de Gran Canaria, Spain:  
591 2011, p. 1–6.
- 592 [17] Sarmah N, Richards BS, Mallick TK. Design, development and indoor performance analysis  
593 of a low concentrating dielectric photovoltaic module. *Solar Energy* 2014;103:390–401.

- 594 [18] Abu-Bakar SH, Muhammad-Sukki F, Ramirez-Iniguez R, Mallick TK, Munir AB, Mohd  
595 Yasin SH, et al. Rotationally asymmetrical compound parabolic concentrator for concentrating  
596 photovoltaic applications. *Applied Energy* 2014;136:363–72.
- 597 [19] Abu-Bakar SH, Muhammad-Sukki F, Freier D, Ramirez-Iniguez R, Mallick TK, Munir AB, et  
598 al. Optimisation of the performance of a novel rotationally asymmetrical optical concentrator  
599 design for building integrated photovoltaic system. *Energy* 2015;90:1033–45.
- 600 [20] Ramirez-iniguez R, Muhammad-Sukki F, McMeekin SG, Stewart BG. Optical element. Patent  
601 No. 2497942, 2014.
- 602 [21] Muhammad-Sukki F, Abu-bakar SH, Ramirez-iniguez R, McMeekin SG, Stewart BG, Sarmah  
603 N, et al. Mirror symmetrical dielectric totally internally reflecting concentrator for building  
604 integrated photovoltaic systems. *Applied Energy* 2014;113:32–40.
- 605 [22] Muhammad-Sukki F, Abu-Bakar SH, Ramirez-Iniguez R, McMeekin SG, Stewart BG, Munir  
606 AB, et al. Performance analysis of a mirror symmetrical dielectric totally internally reflecting  
607 concentrator for building integrated photovoltaic systems. *Applied Energy* 2013;111:288–99.
- 608 [23] Messiou A. Y. UK Optical Plastics Ltd. Available from  
609 [Http://www.ukopticalplastics.com/index.html](http://www.ukopticalplastics.com/index.html) Last Accessed on 10 November 2014.
- 610 [24] ARKEMA GROUP. Standard range - Altuglas® acrylic resins. Available from  
611 [Http://www.altuglas.com/en/resins/resins-by-Performance/standard-Range/index.html](http://www.altuglas.com/en/resins/resins-by-Performance/standard-Range/index.html) - LAs  
612 t Accessed on 10 Nov 2014.
- 613 [25] Sarmah N. Design and Performance Evaluation of a Low Concentrating Line-axis Dielectric  
614 Photovoltaic System. PhD Thesis, Heriot-Watt University, United Kingdom, 2012.
- 615 [26] Solar Capture Technologies. Cells. Available from  
616 [Http://solarcapturetechnologies.com/services/manufacturing/cells](http://solarcapturetechnologies.com/services/manufacturing/cells) Last Accessed on 10 Nov  
617 2014.
- 618 [27] Kempe MD. Accelerated UV test methods and selection criteria for encapsulants of  
619 photovoltaic modules. 2008 33rd IEEE Photovoltaic Specialists Conference, IEEE; 2008, p. 1–  
620 6.
- 621 [28] Volker Quaschnig. *Understanding Renewable Energy Systems*. Earthscan; 2004.
- 622 [29] Ning X, Winston R, O’Gallagher J. Dielectric totally internally reflecting concentrators.  
623 *Applied Optics* 1987;26:300–5.
- 624 [30] Mammo ED, Sellami N, Mallick TK. Performance analysis of a reflective 3D crossed  
625 compound parabolic concentrating photovoltaic system for building façade integration.  
626 *Progress in Photovoltaics: Research and Applications* 2013;21:1095–103.
- 627 [31] Hankins M. *Stand-alone Solar Electric Systems: The Earthscan Expert Handbook for  
628 Planning, Design and Installation*. Earthscan; 2010.
- 629 [32] University of Oregon USA. Sun path chart program. Availabe from  
630 <http://solardat.uoregon.edu/SunChartProgram.html> Last Accessed on 10 June 2014.

- 631 [33] Kumar R, Rosen MA. A critical review of photovoltaic–thermal solar collectors for air  
632 heating. *Applied Energy* 2011;88:3603–14.
- 633 [34] X-Rates. 2014. Currency Calculator. Available from <http://www.x-rates.com/calculator/>. Last  
634 accessed on 10 March 2014.
- 635 [35] Welford WT, Winston R. *High Collection Nonimaging Optics*. Academic Press; 1989.
- 636 [36] MojoCorp Ltd. 2015. Common window sizes. Available from  
637 <http://www.simplifydiy.com/windows-and-doors/windows/window-sizes>. Last accessed on 20  
638 December 2015.
- 639 [37] Solanki CS. *Solar Photovoltaics: Fundamentals, Technologies And Applications*. 3rd ed. PHI  
640 Learning; 2015.
- 641 [38] Sendhil Kumar N, Matty K, Rita E, Simon W, Ortrun A, Alex C, et al. Experimental validation  
642 of a heat transfer model for concentrating photovoltaic system. *Applied Thermal Engineering*  
643 2012;33-34:175–82.
- 644 [39] Sellami N. *Design and characterisation of a novel translucent solar concentrator*. PhD Thesis,  
645 Heriot-Watt University, United Kingdom, 2013.
- 646